Indian J. Phys. **66B** (5& 6), 583–591 (1992)

Continuum radiation due to collective plasma process in quasars

R T Gangadhara and V Krishan
Indian Institute of Astrophysics, Bangalore-560 034, India

Abstract : There are three ways in which an electromagnetic wave can undergo scattering in a plasma : (i) when the scattering of radiation occurs by single electron, it is called Compton Scattering (CS); (ii) if it occurs by longitudinal electron plasma mode, it is called Stimulated Raman Scattering (SRS); and (iii) if it occurs by a highly damped electron plasma mode, it is called Stimulated Compton Scattering (SCS). The nonthermal continuum of quasars is believed to be produced through the combined action of synchrotron and inverse Compton processes, which are essentially single processes. Here, we investigate the role of SRS ans SCS in the generation of continuum radiation from these compact objects. It is shown as an example that the complete spectrum of 3C 273 can be reproduced by suitably combining SCS and SRS. The differential contributions of SCS and SRS under different values of the plasma parameters are also calculated.

Keywords : Plasma instability, 3C 273-spectrum, quasar, Raman scattering, Compton scattering.

PACS Nos. : 98.54.Aj, 52.35.—g.

1. Introduction

One of the most challenging problems in the area of active galactic nuclei (AGN) is the mechanism of continuum emission. In the broadest sense, the important issues are mechanisms responsible for the radiation, the kinematics and the spatial distribution of the continuum emitting regions, and the connection of the continuum emission to the central engine. A surprisingly large number of plausible explanations for the origin of this continuum have involved incoherent radiation mechanisms. The most common is synchrotron self-Compton emission from nonthermal electrons, which seems to work rather well from the IR to UV, particularly for blazars [1,2]. But the Comptonized, self-absorbed thermal cyclotron radiation from mildly relativistic electron beam also appears to be able to fit that part of the spectrum [3]. A sequence of plasma processes, in order to account for the energy gain and loss of electron beam, has been discussed by Krishan and Wiita [4,5]. In this paper we investigate the scattering of the incident (pump) electromagnetic wave off the electron plasma wave in the two regions namely SRS and SCS, and estimate the contribution of these processes in the generation of complete spectrum from radio to X-rays.

2. Stimulated Compton and Raman scattering as energy loss mechanisms

We begin with standard model consisting of a black hole of mass $M = 10^8 M_{\odot}$ surrounded by relativistic plasma which extends to few times Schwarzschild radius R_s, ($R_s = GM/c^2$) and produces the nonthermal continuum. The nonthermal polarized low frequency electromagnetic wave (soft-photon) is considered as a pump which drives parametric instabilities. This soft-photon field may be identified with the cyclotron or synchrotron radiation [2,5]. Our model consists of electron beam which propagates radially outwards and interacts with the soft-photon field to produce radiation at higher frequencies. The generation and stability of extremely sharp electron beams in the quasar environment has been discussed by Lesch *et al* [6].

2.1. *Lorentz transformations* :

Since it is much simpler to do the nonrelativistic calculations in the beam frame, we compute growth rates and the scattered flux in the beam frame and then transfer these quantities to laboratory frame.

Consider and electron beam moving in the z-direction. We use prime on the quantities in the beam frame to distinguish them from the quantities without prime in the laboratory frame. The invariance of phase of an electromagnetic wave gives

$$k_i' \cdot r - \omega_i' t' = k_i \cdot r - \omega_i t. \tag{1}$$

The eq. (1) implies

$$k_x' = k_x,\ k_y' = k_y,\ k_z' = \gamma\left(k_z - \frac{\vartheta_b}{c^2}\omega_i\right) \text{ and } \omega_i' = \gamma(\omega_i - k_z \vartheta_b). \tag{2}$$

where ϑ_b and $g = 1/\sqrt{1 - \vartheta_b^2/c^2}$ are the beam velocity and Lorentz factor, respectively.

Since Lorentz contraction increases the density by γ and the mass also by a factor γ, the plasma frequency ω_p $(=4\text{p}n_e e^2/m_e)^{1/2}$ (where e is the electron charge, n_e the beam density and m_e the electron mass) is frame invariant.

The thermal speed ϑ_T in the beam frame can be expressed in terms of the energy spread of the beam in the laboratory frame and is given by :

$$\vartheta_T = c\frac{\Delta\gamma}{\gamma}. \tag{3}$$

We now consider the transformation of the growth rate Γ. If a wave with slowly varying amplitude $A'(z',t')$ grows in time and space at a temporal growth rate Γ' in the beam frame then A satisfies the following equation

$$\frac{\partial A'}{\partial t'} + \vartheta_g' \frac{\partial A'}{\partial z'} = \Gamma' A', \tag{4}$$

where ϑ_g is the group velocity in the beam frame. The Lorentz transformation of the eq. (4) gives :

$$\Gamma = \frac{\Gamma'}{\gamma\left(1+\vartheta_b\vartheta_s'/c^2\right)} \approx \frac{\Gamma'}{2\gamma}. \tag{5}$$

2.2. Stimulated Compton or stimulated Raman scattering :

Consider a large amplitude plane polarized electromagnetic pump wave,

$$E_i' = 2E_i'\mathrm{Cos}(k_i'\cdot r' - \omega_i't')\hat{x}', \tag{6}$$

propagating in a homogeneous plasma. In the equilibrium, electrons oscillate with velocity ϑ_i in the pump field E_i'. Here, we consider a special case of parametric instability in which the high-frequency side-band modes are predominantly electromagnetic so we essentially have the problem of stimulated scattering where pump (electromagnetic) wave excites an electron plasma wave (ω_l', k_l') and two new electromagnetic waves at shifted frequencies : Stokes mode (ω_s', k_s') and anti-Stokes mode (ω_{as}', k_{as}'). The instability resonantly excites only when the following phase matching conditions are satisfied

$$\omega_i' = \omega_s' + \omega_l', \; k_i' = k_s' + k_l', \tag{7}$$

$$\omega_i' + \omega_l' = \omega_{as}', \; k_i' + k_l' = k_{as}'. \tag{8}$$

Each of the excited modes satisfies its own linear dispersion relation in the plasma medium. If we solve the dispersion relation of the electron plasma wave in the beam frame [7], we have

$$\omega_l' \approx \omega_p \qquad \text{for} \quad k_l'\lambda_D' << 0.4; \tag{9}$$

$$\omega_l' \approx k_l'\vartheta_T[1 - io(1)] \quad \text{for} \quad k_l'\lambda_D' \geq 0.4, \tag{10}$$

where $V_T = \left[(2/n_e')\int_{-\infty}^{+\infty} v^2 f_e dv\right]^{1/2}$ and $\lambda_D' = \left(k_B T_e / 4\pi n_e' e^2\right)^{1/2}$ are the thermal speed and Debye length of the electron plasma, respectively (k_B = Boltzman constant). Eq. (10) indicates that if $k_l'\lambda_D'$ larger than or equal to 0.4 then the electron plasma mode losses its wave nature because of its large Landau damping.

The dispersion relation of the electromagnetic wave in a plasma is

$$\omega'^2 = \omega_p^2 + k'^2c^2. \tag{11}$$

The pump wave, the Stokes mode and the anti-Stokes mode satisfy the dispersion relation (11) in the plasma medium. If the pump wave undergoes backscattering and for $(\omega_i', \omega_s') >> \omega_p$ and $k_i' \approx k_s'$ then $k_l' = k_s'$. Hence for a given quality of a beam, if ω_s' is increased by increasing pump frequency ω_i', k_l' which may be initially smaller than $0.4/\lambda_D'$ becomes larger than $0.4/\lambda_D'$ at some value of ω_s' . Hence, there exists a critical frequency of the scattered wave above which the scattering process is Compton and below which it becomes Raman. If we write this critical angular frequency in the laboratory frame as ω_{cr}, it can be expressed in terms of beam quality. Using $\omega_{cr} \approx 2\gamma\omega_s', \omega_s' \approx ck_s'$ and $k_l' = 2k_s' = 0.4/\lambda_D'$ we have, with eq.(3) :

$$\omega_{cr} = 0.4\sqrt{2}\,\gamma\,\omega_p \frac{\gamma}{\Delta\gamma} \tag{12}$$

Thus the critical frequency depends on the relative spread $\Delta\gamma/\gamma$ of the beam energy observed in the laboratory frame, as well as the beam density n_e and γ.

2.3. *Growth rates of stimulated Raman and Compton scattering :*

The most general plasma dispersion relation to describe parametric instability excited in plasma medium by a large amplitude coherent electromagnetic wave, has been derived by Drake *et al* [8] using Vlasov equation. If the excited side-band modes are predominantly electromagnetic then it reduces to

$$1+\frac{1}{\chi_e'(k',\omega')}=k'^2\left[\frac{|k_-'\times\vartheta_i'|^2}{k_-'^2D_-}+\frac{|k_+'\times\vartheta_i'|^2}{k_+'^2D_+}\right], \tag{13}$$

where $\vartheta_i'=eE_i'/m_e'\omega_i'$ is the quiver velocity of electrons, $\chi_e'(k',\omega')$ the electron susceptibility function, $\omega_\pm'=\omega_i'\pm\omega', k_\pm'=k_i'k'$ and

$$\begin{aligned} D_\pm &= c^2k_\pm'^2-\omega_\pm'^2+\omega_p^2 \\ &= c^2k'^2\pm 2k'\cdot k_i'c^2\mp 2\omega'\omega_i'-\omega'^2 \end{aligned} \tag{14}$$

In the eq. (13), when the three wave interaction is resonant then ω' and k' becomes the angular frequency and wave vector of the electron plasma wave (ω_l',k_l'). In the case of backscattering, $\left(\phi_s'=\cos^{-1}\left(\hat{k}_i'\cdot\hat{k}_s'\right)=180^\circ\right), D_-\approx 0$ and $D_+\neq 0$, only Stokes mode excites but not the anti-Stokes mode. But in the case of right angle scattering $\left(\phi_s'=90^\circ\right)$ both $D_-\approx 0$ both and $D_+\approx 0$ and hence both the modes are excited. The anti-Stokes mode does not excite for $\omega'<<\left(c^2k_i'\cdot k_l'/\omega_i'\right)$ and it is excited only when k' is very small or if k'_l is nearly perpendicular to k'_i.

2.4. *Numerical solution of equation (13) :*

When $\omega_l'\approx\omega_p\le k_l'\vartheta_T$ or $k_l'\lambda_D'\approx 0.4$, it is not possible to expand $\chi_e'(\omega',k')$ in to an asymptotic series. Therefore, using $\omega'=\omega_l'+i\Gamma'$ we numerically solve eq. (13) including all the damping effects. If we separate real and imaginary parts of eq. (13) we get two coupled equations. To find ω'_l and Γ', we solve these two equations with the relation of Fried and Conte's plasma dispersion function [9] and its relation with the error function. We have to find the value of k'_l such that it satisfies (7), (8), the dispersion relation of electron plasma mode and $D_-\approx 0$.

We assume the power laws spatial variation along the path of the beam for electron density n_e, Lorentz factor γ, pump frequency ν'_i and the pump flux $f_{\nu i}$ to calculate growth rate Γ' and the scattered flux $f_{\nu s}$ (calculated in the next section). We find the following power laws give a fairly good agreement with the observed spectrum in the case of 3C 273. The density of relativistic electron beam follows the power law given by :

$$n_e = n_0\left(\frac{r}{r_0}\right)^{-3.2} \tag{15}$$

where $n_0 = 9.24 \times 10^{17}\ \mathrm{cm}^{-3}$ and $r_0 = 10R_s = 1.4767 \times 10^{14}$ cm for black hole of mass $M = 10^8 M_\odot$. In the beam frame, an electron density is given by $n'_e = n_e / \gamma$. The frequency and flux of the soft-photon field are assumed to follow the power laws given by :

$$\nu_i = \nu_0\left(\frac{r}{r_0}\right)^{-1.0} \tag{16}$$

where $\nu_0 = 4 \times 10^{10}$ Hz and

$$f_{\nu i} = f_0\left(\frac{\nu_i}{\nu_0}\right)^{-0.1} \tag{17}$$

where $f_0 = 7.1 \times 10^{-25}$ erg cm^{-2} sec^{-1} Hz^{-1}. Thus we study the scattering of this low frequency ($\nu_i = \omega_i/2\pi$) wave with the beam electrons through the processes SRS and SCS. Here we find that even though $\omega_i < \omega_p, \omega'_i > \omega_p$ for $\hat{k}'_i = -\hat{z}'$. Therefore, it suffices to take $\omega_i \leq \omega_p$ for $\gamma > 1$ for the present calculations. The power law for Lorentz factor is assumed to be :

$$\gamma = \gamma_0\left(\frac{r}{r_0}\right)^{-1.2} \tag{18}$$

where $\gamma_0 = 3 \times 10^3$. We observe that in the beam frame the plasma expands uniformly with the density proportional to r^{-2}. The spread in energy of the beam $\Delta\gamma/\gamma$ is assumed to remain constant through out its path. Also, we assume the scattered radiation has the same polarization as the incident one ($\vartheta'_s = 0$).

3. Limiting gain and output power

The scattered radiation fields E'_s and B'_s become large as the instability progresses. At the critical frequency (eq. 12) the Lorentz force $\vartheta'_i \times B'_s$ begins to act on electrons. The associated electric potential traps the beam electrons which results in an increase in their thermal spread. The trapping potential ϕ'_t due to Lorentz force $\vartheta'_i \times B'_s$ in the beam frame is obtained from

$$\left|\frac{\partial \phi'_t}{\partial z'}\right| = \left|k'_i \phi'_t\right| \approx \frac{1}{c}\left|\vartheta'_i B'^{*}_s\right|$$

given by :

$$\phi'_t = \frac{1}{k'_i}\frac{|\vartheta'_i|}{c}|B'_s|. \tag{19}$$

The effective thermal speed ϑ_{Teff} due to the trapping potential is

$$\vartheta_{Teff} = \left(2e\phi'_t / m_e\right)^{1/2} \tag{20}$$

The growth rate of the instability reaches the maximum $(\Gamma' = \Gamma'_m)$ at the critical frequency (eq. 12) when $k'_l = \omega_p/\vartheta_{Teff}$ (Figure 1) because for $\vartheta_{Teff} \geq \omega_p / k'_l$ Landau damping begins begins to play a dominant role and the gain changes from Raman to Compton. The scattered radiation magnetic field, at the critical frequency, is given by :

$$B'_{sm} = \left(\frac{m'_e}{2e}\right)\frac{c}{\vartheta'_i}\frac{\omega_p^2}{k'_l} \tag{21}$$

The growth of the scattered radiation magnetic field B'_s is governed by the equation :

$$\frac{dB'_s}{dt'} = \Gamma' B'_s, \tag{22}$$

where Γ' is the growth rate in the beam frame. Integrating (22) we get

$$B'_s(t') = C_1 \mathrm{Exp}[\Gamma' t']. \tag{23}$$

At $\Gamma' = \Gamma'_m, B'_s = B'_{sm}$, we find the flux emitted during the characteristic time $t' = 1/\Gamma'_m$. Using (23), the flux of scattered radiation in the beam frame is given by :

$$S' = \frac{c}{4\pi} B'^2_{sm} \exp\left[2\left(\frac{\Gamma'}{\Gamma'_m} - 1\right)\right]. \tag{24}$$

To transfer flux to the laboratory frame, first we resolve E'_s and B'_s into components $E'_{s\parallel}$ and $B'_{s\parallel}$ parallel, and $B'_{s\perp}$ and $E'_{s\perp}$ perpendicular to $\hat{z}'$. Taking E'_s, E'_i along $\hat{x}'$ the components of E'_s and B'_s are given by :

$$B'_{s\perp} = -B'_s \cos(\phi'_s)\hat{y}', \quad E'_{s\perp} = E'_s \hat{x}', \tag{25}$$

$$B'_{s\parallel} = -B'_s \sin(\phi'_s)\hat{z}', \quad E'_{s\parallel} = 0,$$

where $\phi'_s = \cos^{-1}\left(\hat{k}'_i \cdot \hat{k}'_s\right)$. Now, components of the flux vector in the laboratory frame are given by :

$$S_\perp = \frac{c}{4\pi}\gamma^2 B'^2_{sm} \exp\left[2\left(\frac{\Gamma'}{\Gamma'_m} - 1\right)\right]\left[\left(1 + \cos^2(\phi'_s)\right)\frac{\vartheta_b}{c} - \left(1 + \frac{\vartheta_b^2}{c^2}\right)\cos(\phi'_s)\right]\hat{z}', \tag{26}$$

$$S_\perp = \frac{c}{4\pi}\gamma B'^2_{sm} \exp\left[2\left(\frac{\Gamma'}{\Gamma'_m} - 1\right)\right]\left[1 - \frac{\vartheta_b}{c}\cos(\phi'_s)\right]\sin(\phi'_s)\hat{y}'. \tag{27}$$

If the pump field strength is increased it produces a spread in the beam velocity, consequently it decreases the scattered power and increases the growth rate. The scattered radiation gains all its energy from the relativistic electron beam. Consequently, the electron beam gets decelerated due to the interaction with the pump. The emitted radiation is beamed and confined to a cone of angular radius $\approx 1/\gamma$. The scattered radiation flux, at the observer, is given by :

$$f_{\nu s} = \frac{1}{2}\left(\frac{R_b}{R_e}\right)^2 \frac{S}{\nu_s}, \tag{28}$$

where $S = \left[S_{\parallel}^2 + S_{\perp}^2\right]^{1/2}$, $R_b = r\tan(\Delta\theta)$ the radius of the beam at a distance of $r \geq 10R_s$ from the central engine $\Delta\theta$ the angular radius of the beam and $R_e = 7.9 \times 10^8$ pc the distance between quasar 3C 273 and the earth. Using the observed value of the flux of 3C 273 at 10^{18} Hz we fix $\Delta\theta = 0.0065°$. We calculate the scattered flux at other frequencies using the spatial variation of plasma parameters as discussed earlier. Thus R_b increases as r increases for constant $\Delta\theta$ = constant at all frequencies.

3.1. Discussion and figure description :

Figure 1. This figure shows the growth rate as a function of the frequency ν_s of the backscattered radiation for three different values of initial density : n_0, $n_0/2$ and $2n_0$, using the different power laws given on figure. First consider the curve labelled with n_0, in the range $10^{10} \leq \nu_s \leq 10^{13.85}$ Hz, the growth rate of the backscattering of electromagnetic radiation increases with ν_s and reaches maximum at $\nu_s = 10^{13.85}$ Hz.

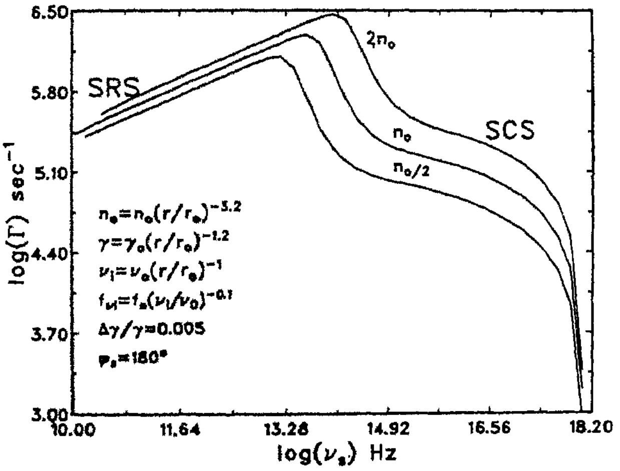

Figure 1. Growth rate Γ versus scattered wave frequency ν_s at three different values of electron density in the laboratory frame. At maxima, the scattering process changes from SRS to SCS. The constants are : $\gamma_0 = 3 \times 10^3$, $n_0 = 9.24\ 10^{17}$ cm^{-3}, $\nu_0 = 4 \times 10^{10}$ Hz and $f_0 = 7.1 \times 10^{-25}$ erg cm^{-2} sec^{-1} Hz^{-1}.

As ν_s is further increased, electron plasma mode experiences a large Landau damping because $k_l'\lambda_D' > 0.4$, and in the range $10^{13.85} \leq \nu_s \leq 10^{14.7}$ Hz, growth rate decreases rapidly with ν_s. Further in the range $10^{14.7} < \nu_s \leq 10^{17}$ Hz, due to the saturation of Landau damping, growth rate shows slow decrease. For $\nu_s > 10^{17}$ Hz, which occurs rather in the high density region, collisional damping rate of electron plasma mode becomes large, resulting in sharp decrease in the growth rate. The frequency of the scattered radiation corresponding to maximum growth rate, the critical frequency ν_{cr} acquires higher values with an increase in density. The scattered radiation of frequency below ν_{cr} produced due to the SRS ans above due to SCS.

Figure 2. Here the theoretical spectrum of the backscattered and incident radiations are plotted (continuous curves). For comparison we have also shown observed points (o-points represent spectrum of 3C 273, when flare activity was going on during February, 1984 and Δ-points represent its normal spectrum observed during February, 1986) by quasi-simultaneous multifrequency observations of Courvosier *et al* [10]. At the critical frequency $\nu_s = 10^{13.85}$ Hz, there is a break in the spectrum due to the change of scattering process from SRS to SCS. The SRS process contributes in the lower frequency part of the spectrum ($\nu_s \leq 10^{13.85}$) while SCS contributes in the higher energy part. The slope of the spectrum in the SRS region is –0.8 and in the SCS region it is –0.7. The hard X-ray part of the spectrum is steep due to collisional damping and the slope of this part is –1.5. The bump in the spectrum is produced at the transition region $\left(k_i'\lambda_D' = 0.4\right)$ between the SRS ans SCS regions.

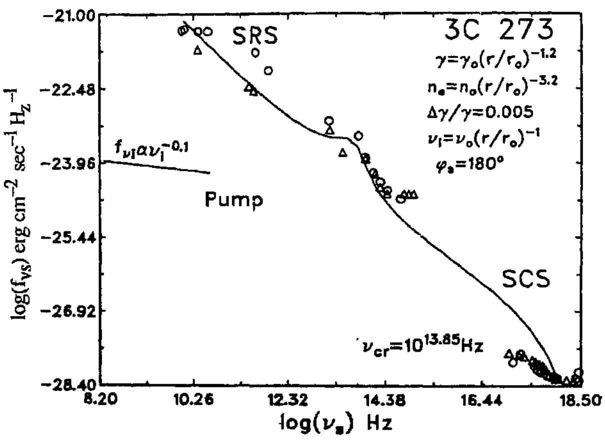

Figure 2. The spectrum of quasar 3C 273. The solid lines represent the calculated spectrum and the spectrum of the pump wave. The observed points, O-(February, 1984) and Δ-(February, 1986) by Courvoisier *et al* [10], are also plotted. The constants are : $\gamma_0 = 3 \times 10^3$, $n_0 = 9.24 \times 10^{17}$ cm^{-3}, $\nu_0 = 4 \times 10^{10}$ Hz.

4. Conclusions

(1) Compared to Compton scattering, Raman scattering is a faster process.

(2) At higher plasma density n_e and lower energy spread $\Delta\gamma/\gamma$, Raman scattering can produce the entire continuum radiation right from radio to X-rays.

(3) Similarly, at lower density and higher energy spread $\Delta\gamma/\gamma$, Compton scattering can produce the entire continuum radiation right from radio to X-rays.

(4) For the parameters chosen here, the transition region between SRS and SCS lies where the bump is observed for 3C 273. Thus, we suggest the change of scattering process as one of the possible causes for the spectral break, observed in the most of the quasars and AGN.

(5) Raman scattering occurs in a region of density greater than or equal to quarter critical density $\left(\omega_i' \geq 2\omega_p\right)$

(6) Electron beam gets decelerated much faster due to Raman scattering than due to Compton scattering.

(7) The beamed stimulated Raman or Compton emission can be detected at a small angle to the electron beam axis. The higher frequency radiation is produced in a narrow angular region around the electron beam axis than the lower frequency radiation.

(8) As we see the scattering processes also bring about polarization changes., which we plan to study in detail.

References

[1] W A Stein and S L O Dell 1985 in *Astrophysics of Active Galaxies and Quasi Stellar Objects,* ed. J S Miller (Mill Valley : University Science Books) p 381

[2] W A Stein 1988 in *Active Galactic Nuclei*, eds. H R Miller and P J Wiita (Heidelberg : Springer Verlag) p 188

[3] M C Begelman 1988 in *Active Galactic Nuclei,* eds. H R Miller and P J Wiita (Heidelberg : Springer Verlag), p 202

[4] V Krishan and P J Wiita 1986 in *IAU symp.* No. 199 on *Quasar*, eds. G Swarup and V K Kapahi (Dordrecht : Reidel) p 419

[5] V Krishan and P J Wiita 1990 *Mon. Not. R. A. S.* **246** 597

[6] H Lesch, R Schlickeiser and A Crusius 1988 *Astrophys.* **200** L9-L12

[7] A Hasegawa 1978 *Bell System Tech. J.* **57** 3069

[8] J F Drake, P K Kaw, Y C Lee, G Schmidt, C S Liu and M N Rosenbluth 1974 *Phys. Fluids.* **17** 778

[9] D Fried and S D Conte 1961 *The Plasmsa Dispersion Function* (New York : Academic)

[10] T J-L Courvoisier, M J L Turner, E I Robson, W K Gear, R Staubert, A Blecha, P Bouchet, R Falomo, M Valtonen and H Teräsranta 1987 *Astron. Astrophys.* **176** 197